- Technical Paper -

EXPERIMENTAL INVESTIGATION OF REINFORCED CONCRETE COLUMNS RETROFITTED BY THICK HYBRID WING-WALL

Mohammad Zahid NOORI[*1], Kozo NAKADA[*2], Kazuo KANEDA[*3], Tetsuo YAMAKAWA[*4]

ABSTRACT

Thick Hybrid Wall (THW) is a strength–ductility type seismic retrofit technique composed of an existing reinforced concrete (RC) column and an additional wall united by a channel–shaped steel plate and PC bars for vulnerable soft first–story RC buildings. The shear and flexural strength improvement in the THW section by adjusting minimum additional wall length and the section's unity are experimentally investigated by testing four THW specimens. Shear and flexural strength improvement by the THW technique was verified and the section's monolithic behavior was observed.

Keywords: Seismic retrofit, Prestress, Wing-wall, Flexural strength, Shear strength

1. INTRODUCTION

Seismic hazards are unpredictable and induce the most dangerous disasters in countries with high seismic profiles. In Japan, the earthquake has induced devastating damages on the various type of buildings. The existing soft first-story type RC building is among these seismically vulnerable buildings due to formation of soft-story mechanism as consequence of strength and stiffness irregularities. The seismic performance records of soft first-story RC buildings against the Hyogo-ken–Nanbu and the Kumamoto earthquakes indicate their seismic vulnerability dimensions. This type of building has massively constructed in many countries with high seismic profiles and needs to be seismically assessed and retrofitted. In response to seismic vulnerability of this type of buildings, Yamakawa [1] proposed seismic retrofit of RC columns confined by PC bars. Thereafter, THW technique was proposed in ref. [2] in 2007.

THW technique is based on adjusting a same thickness concrete wing or panel-wall into an existing RC column jacketed by channel-shaped steel plate and tightened by high-strength PC bars. The same-thickness additional wall is applied to provide a uniform outer surface and PC bars are used to tight the THW element. Seismic performance of the retrofitted THW element improves due to the involvement of the existing RC column, additional wall, steel plate and PC bars. These components combinedly function as shear and flexural resistant element. Thus, the flexural strength improves by increasing internal lever arm and yielding of rebars as consequence of shifting neutral axis to the additional wall side when the additional wall is under compression. Shear strength improves by diagonal compressive strut depth increase and by contribution of steel plate and PC bars as shear reinforcement in the THW element.

The active lateral confinement effectiveness by PC bars on the compressive strength and shear resistance mechanism of the section was experimentally evaluated by Nakada and Yamakawa [3, 4]. The lateral confinement by PC bars is a key point which THW is based on. Two models of shear transition mechanisms for the retrofitted THW element were proposed in two studies by (Rahman and Yamakawa) [2] and, by (Pasha and Yamakawa) [5]. Rahman's model is a combination of truss and arch as shear transition mechanism but, Pasha's model neglected the truss mechanism from the safety and simplification perspectives. However, these models result different strength for the same specimen. A simplified equation was proposed for calculation of flexural strength in the THW element in ref. [2]. It was modified by replacing concrete compressive strength of RC column to that of additional concrete in ref. [5].

In another study on the flexural strength of retrofitted THW element by Nakada [6], two equations are proposed to calculate ultimate flexural strength and determine minimum additional wall length ratio. The proposed equation calculates ultimate flexural strength regardless of the axial force limitations compared to the simplified equation in ref. [5]. These equations are based on an assumption that the existing RC column and additional wall behave as a monolithic element in order to meet the flexural assumptions of ref. [7].

In this experimental investigation, four THW specimens (R19W-5FB, R19W-7FB, R19W-5SU, R19W-7SU) are tested to evaluate shear and flexural strengths improvements when minimum additional wall length is considered in the THW element. The flexural strength is evaluated by testing of 5FB and 7FB specimens. The shear strength is evaluated by testing of 5FB, 7FB, 5SU, and 7SU specimens. Contribution of steel plate and PC bars as unifiers of the THW element is discussed to experimentally evaluate the monolithic behavior of THW element.

*1 Grad. Sch. of Eng. & Sci., Univ. of the Ryukyus, M.Eng., JCI Student Member
*2 Associate Prof., Faculty of Engineering, Univ. of the Ryukyus, Dr. Eng., JCI Member
*3 Prof., National Institute of Technology, Ariake College, Dr. Eng., JCI Member
*4 Emeritus Prof., Univ. of the Ryukyus, Dr. Eng., JCI Member

2. TEST PLAN

Two types of bond (5FB and 7FB) and unbond (5SU and 7SU) specimens were constructed to experimentally evaluate the strength improvement by applying THW technique. Unbonded specimens were constructed to evaluate shear transition by the arch mechanism. Thus, the bond force between longitudinal rebars and concrete were removed in these specimens via embedding longitudinal rebars within plastic tubes. Both bond and unbond specimens were composed of an existing RC column and additional wall united by a channel-shaped steel plate and tightened by PC bars. The retrofitted THW specimens were rigidly connected by two RC stubs at their top and bottoms.

The sectional dimensions of the existing RC column were (b = D = 250 mm) and its ratio of shear span to clear height (H = 750 mm) was 1.5. The RC column section was reinforced with 12-D10 rebars and low-strength transverse reinforcement hoops ϕ3.7 spaced @105 mm to minimize the hoops' contribution in the truss mechanism (to fail the existing RC column by shear). Concrete was cast in two steps. The existing RC column was monolithically casted with two stubs (length = 1600 mm, width = 480 mm, height = 500 mm) in the first step. The additional concrete was cast in the second step within the steel plate after hardening of casted concrete in the first step. The gap between existing RC column and the steel plate's inner surface t_{add} was 30 mm which was filled by additional concrete during the concrete cast of the additional wall. The structural details of the retrofitted THW specimens are illustrated in Fig 1.

The specimens were constructed with two additional wall length ratios (β = 0.55 and β = 0.75). The value β = 0.55 was obtained by the minimum additional wall length ratio calculation equation. The value β = 0.75 was selected to evaluate the increase level of ultimate strength in comparison to the value β = 0.55. For the specimens with β = 0.55, 6-13ϕ PC bars were arranged in one vertical row, and for the specimens with β = 0.75, 12-13ϕ PC bars were arranged in two vertical rows. Since the steel plate thickness and material properties of the unbond specimens were the same, the difference in their shear strength would be due to the variation in concrete compressive strut depth k and arch angle θ. Bond specimens 5FB and 7FB were built to experimentally verify the ultimate flexural strength in the retrofitted THW section when minimum additional wall length was considered. The test specimens' details and their material properties are illustrated in Table1 and in Table2 respectively. The steel plate's thickness (t = 3.2 mm), applied tensile strain on the PC bars (ε_{pt} =1000 μ) and the distribution of PC bars in the additional wall (6-13ϕ and 12-13ϕ) were selected based on the previous research (on the testing of THW specimens in ref. [2]).

As shown in Fig. 2, two types of strain gages (uniaxial and triaxial) were attached on the surface of steel plates to measure the shear stress carried by the steel plates. Uniaxial strain gages were attached on the surface of three PC bars in specimens with additional wall length ratio of β = 0.55. Six uniaxial strain gages were attached on the surface of PC bars in specimens with additional wall length ratio β = 0.75. PC bars with attached strain gages were embodied at the top, center, and bottom of the additional wall.

Applied initial tensile strain on the PC bars was 1000 μ and carried out by hand on the PC bars with and without attached strain gages. On the PC bars without attached strain gages, tensile strain was applied by twisting the PC bars' nuts to the same angle as the PC bars with attached strain gages. The approximate twist of the PC bars' nuts varied between 170° to 220° to apply 1000 μ strain. Tensile strain was carried out after the hardening of additional concrete and just before the loading test. The outer row of PC bars was adjusted close to the exposed surface of wall, thus additional transverse reinforcement was not embodied to confine the exposed surface of wall. The acting axial force ratio (η =$N/bD\sigma_B$) was 0.2. Cyclic loading tests were carried out in one cycle (push and pull) at drift angles (R = 0.125% and R = 0.25%) and, in two cycles at drift angles (R = 0.5%, R = 0.75%, R = 1.0%, R = 1.5%, R = 2.0%, R = 2.5% and R = 3.0%). The test setup and cyclic loading program is shown in Fig. 3.

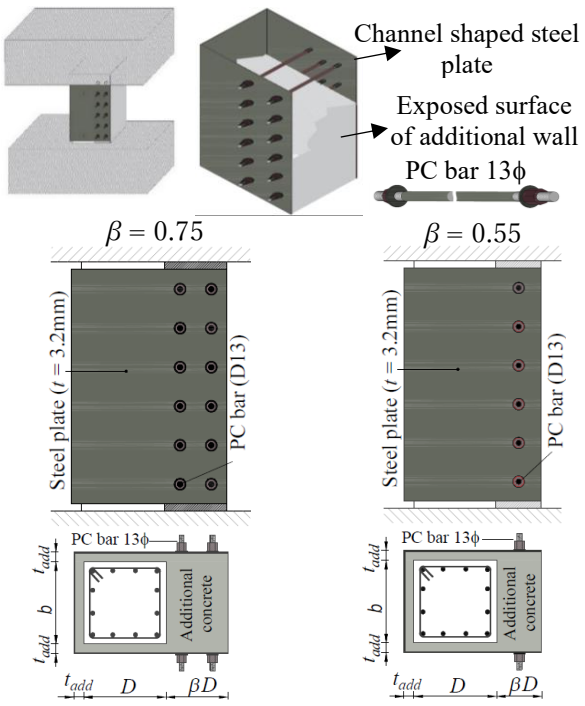

Fig. 1 Structural details of specimens

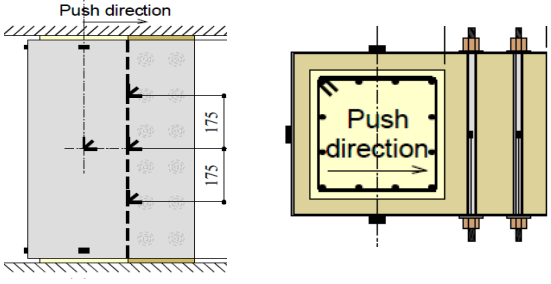

Fig. 2 Schematic position of strain gages

Table 1 Test specimens

No	Specimen (R19W-)	β	ε_{pt} (μ)	t (mm)	Bond or ubnond	Failure mode
1	5FB	0.55	1000	3.2	Bond	Flexure
2	7FB	0.75				
3	5SU	0.55			Unbond	Shear
4	7SU	0.75				
Common details	b =D = 250 mm, $M/(VD)$ = 1.5, H = 750 mm,η = 0.2, (N = 206 kN), σ_B = 16.5 MPa, $\sigma Badd$ = 39.2 MPa, hoop: 3.7ϕ-@105mm, Rebar 12-D10.					

Table 2 Material properties of steel

Steel material		a (cm2)	σ_y (MPa)	Es (GPa)
Rebar	D10	71	393	193
Rebar	D10	71	912	177
Hoops	ϕ3.7	11	268	192
PC bar	ϕ13	132.7	1085	200
Steel plate	t = 3.2mm	-	350	193

Notes: a = cross section area, σ_y = yield strength of steel material and E_s = Young's modulus of elasticity.

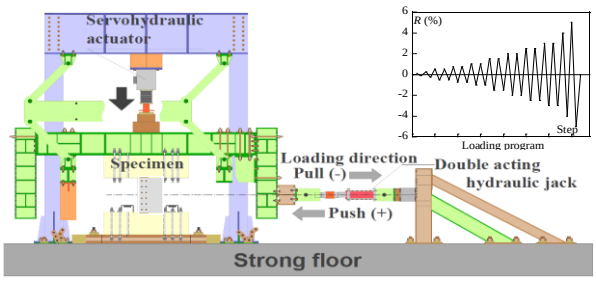

Fig. 3 Test setup and loading program

3. EXPERIMENTAL RESULT AND DISCUSSTION

3.1 Lateral Load V and Drift Angle R Relation

This section is reported based on the experimental data and specimens' observations during the loading test and after steel plate removal at the end of the loading test. The experimental lateral force V and drift angle R curves as well as the detected crack patterns for the specimens are illustrated in Fig. 4 and Fig. 5 respectively.

In bond specimen 5FB (Fig. 4 (a)), the first flexural crack (width = 0.08 mm) appeared at the bottom of the existing RC column at drift angle R = 0.5% in the push direction (bottom of the additional wall is compressed in the push direction and that of the existing RC column is compressed in the pull direction). Longitudinal rebars started to yield at the bottom of the existing RC column at drift angle R = 0.5% as illustrated in Fig. 6 (a). At drift angle R = 1.0%, flexural cracks (width =3 mm) opened throughout the width of the existing RC column at its top and bottom. These cracks enlarged until the specimen's flexural failure due to the formation of plastic hinges at the top and bottom of the existing RC column. Specimen 5FB performed its experimental ultimate lateral strength (V_{max}= 262 kN) at drift angle R = 1.5%. Experimental lateral strength slightly decreased at drift angle R = 2.0%, and 3 mm displacement appeared between the steel plate's edge and the additional wall's exposed surface. Bottom of the additional wall displaced 10 mm at drift angle R = 3.0% and a lateral crack (width = 0.87 mm) appeared in the center of the exposed surface simultaneously. The displacement between additional wall and the existing RC column surface was observed at their boundary line after removing the steel plate.

Bond specimen 7FB (Fig. 4 (b)) started to crack from the top of the exiting RC column at drift angle R = 0.25%. At drift angle R = 0.75%, another flexural crack (width = 2mm) appeared at the bottom of the existing RC column. Longitudinal rebars started to yield at the top of the existing RC column at drift angle R = 0.75% as shown in Fig. 6 (b). At drift angle R = 1.0%, the cracks at the top and bottom of the existing RC column opened (width = 3 mm). Specimen 7FB performed its ultimate lateral strength (V_{max} = 281 kN) at drift angle R = 1.5%. The additional wall displaced 1 mm from the edge of steel plate, and it increased up to 7mm at the end of the loading test. At drift angle R = 3.0%, the lateral strength decreased suddenly due to the tensile breakage of two longitudinal rebars from the bottom of the existing RC column. Vertical spalling of additional concrete was observed throughout the outer row of PC bars by removing the steel plate. This vertical spalling might have occurred due to tensile stress caused by the bending between PC bars and the concrete unconfined area (the area between the exposed surface and PC bars' outer row). This vertical spalling may not have affected the ultimate capacity because it happened right after performing ultimate strength V_{max}.

In unbond specimen 5SU (Fig. 4 (c)), shear crack (width = 1 mm) appeared at the bottom of the additional wall at drift angle R = 0.25%. The top and bottom of the existing RC column cracked at drift angle R = 0.25% in push and pull directions respectively. Shear cracks enlarged at the top and bottom of the existing RC column until drift angle R = 1.5% (when shear failure occurred). Specimen 5SU performed its ultimate lateral capacity (V_{max}= 309 kN) at drift angle R = 1.5%. Displacement between the additional wall and the steel plate's edge was observed when the lateral crack (with = 0.15mm) appeared at the center of the exposed surface. This displacement increased up to 13 mm at drift angle R = 3.0%. At drift angle R = 2.0%, a second lateral crack (width = 0.25mm) appeared at the exposed surface of the additional wall, which indicated formation of a second diagonal crack in the specimen.

In the unbond specimen 7SU (Fig. 4 (d)), a shear crack (width = 0.3 mm) appeared at the bottom of exposed surface in additional wall at drift angle R = 0.25%. This specimen performed its ultimate lateral capacity (V_{max} = 378 kN) at drift angle R = 1.5%. Additional concrete's displacement from the steel plate's edge (width = 2 mm) was observed at drift angle R = 2.0%. A horizontal crack (width = 0.15 mm) appeared at the center of exposed surface at drift angle R = 3.0% and loading test was ended. As illustrated in Fig. 6 (c) and (d), the longitudinal rebars did not yield in the unbond specimens because, they were reinforced by high strength (σ_y= 912 MPa) longitudinal rebars.

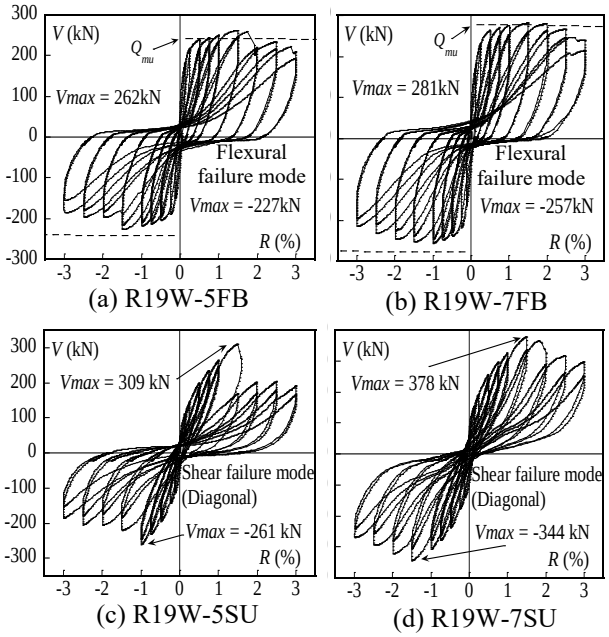

Fig. 4 *V-R* relations

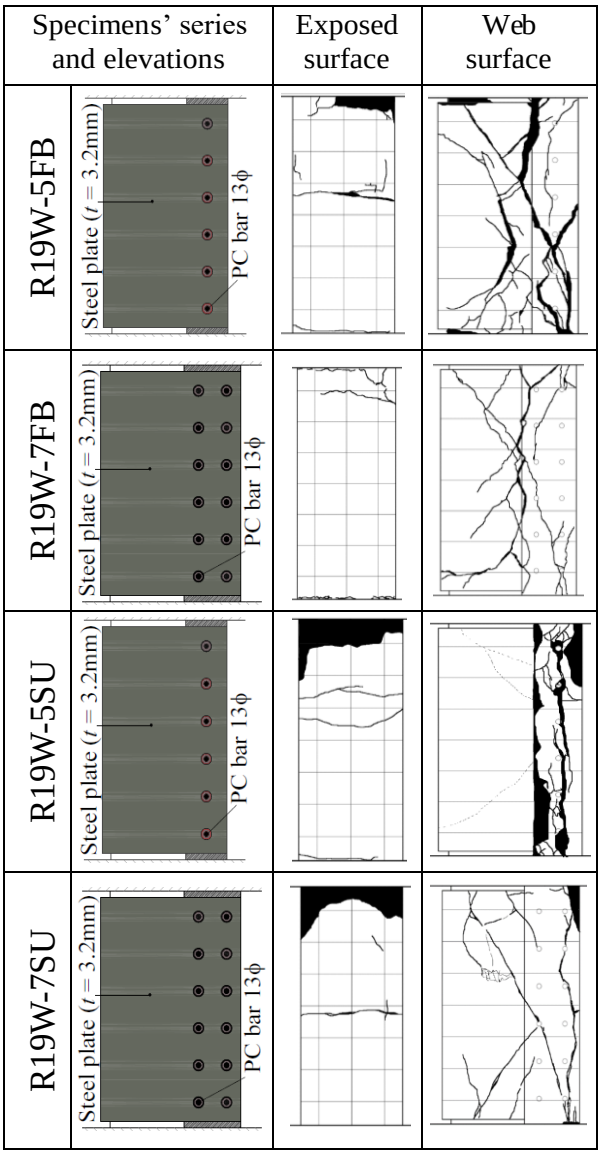

Fig. 5 Detected crack patterns of the specimens

Bond specimens 5FB and 7FB failed in a flexural failure mode due to formation of plastic hinges at the top and bottom of the existing RC column. These specimens failed when all longitudinal rebars yielded in tension in the existing RC column and additional concrete reached to its ultimate compressive strength. Unbonded specimens 5SU and 7SU performed shear failure mode by compressive failure of diagonal compressive strut. Diagonal cracks were observed in unbond specimens when the steel plates were removed at the end of loading test. The observed shear cracks in the center of experimental diagonal compressive struct showed that the diagonal compressive strut reached to its ultimate compressive strength which caused shear failure of unbond specimens. The steel plate and PC bars do not contribute to the truss mechanism of unbond specimens, therefore, the experimental shear strength V_{max} indicates the shear strength of the arch mechanism V_a.

As shown in Fig. 5, continuation of diagonal cracks between the existing RC column and additional wall was observed by removing of steel plate at the end of loading test. There was not any observed evidence of displacement occurred between the existing RC column, additional wall and the steel plate before performing ultimate lateral strength V_{max} during the loading test. Therefore, the existing RC column and additional wall behaved as a monolithic element until performance of ultimate lateral strength V_{max}. On the other hand, the steel plate did not yield in this experiment as shown in Fig. 7. Therefore, the steel plate caused insignificant lateral confinement effect on the diagonal compressive force of unbond specimens and on the compressive resultant force of bond specimens.

The skeleton curves in Fig. 8 indicate that the experimental lateral strength increases by increasing additional wall length ratio β. According to this experiment, the ultimate shear strength V_{max} of unbond specimens was higher than that of the bond specimens with the same additional wall length ratio. On the other hand, the experimental shear strength V_{max} of unbond specimens are higher than the calculated results by the

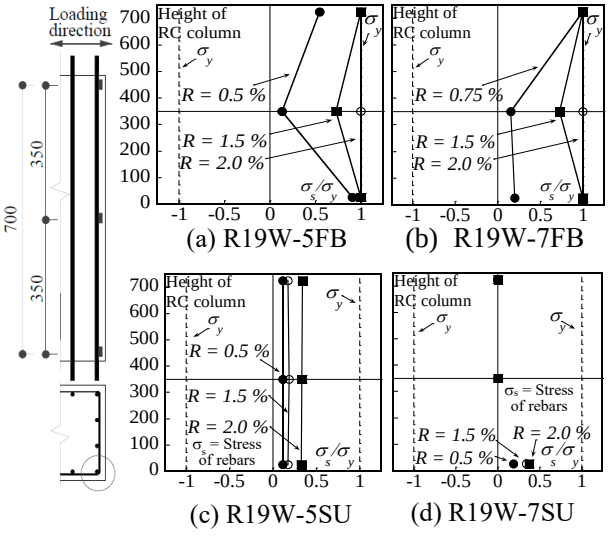

Fig. 6 Stress distribution of longitudinal rebars

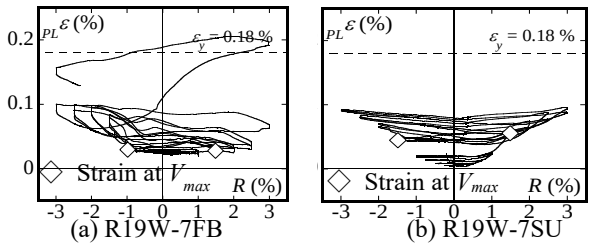

(a) R19W-7FB (b) R19W-7SU

Fig. 7 Strain of steel plate (top of RC column)

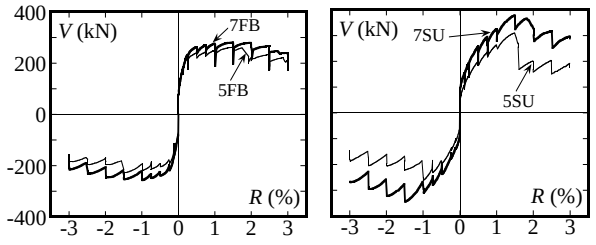

(a) 5FB and 7FB (b) 5SU and 7SU

Fig. 8 Comparison of skeleton curves

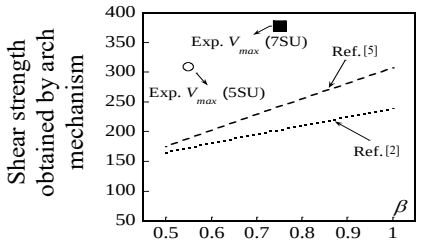

Fig. 9 Comparison of test and calculated results

shear transition models of ref. [2, 5] as is shown in Fig. 9. In the ref. [2], the truss and arch combinedly present the shear transition mechanism for the retrofitted THW element, but only arch mechanism is considered (the truss effect is eliminated for unbond specimens). Arch mechanism presents shear mechanism of the retrofitted THW element in ref. [5]. Fig. 9 indicates that the shear models in ref. [2, 5] do not respond properly to the actual shear strength improvement in the THW element. Therefore, further investigations are needed to develop a proper shear transition mechanism for THW element.

3.2 Flexural Strength

Bond specimens 5FB and 7FB were tested to experimentally evaluate the accuracy of Eq. 1 [6] and the effectiveness of Eq. 2 [6]. Eq. 1 is proposed to calculate ultimate flexural strength based on the ACI stress block parameters when longitudinal rebars yield in the existing RC column and compression zone is in the additional wall side. This equation is based on an assumption that the existing RC column and additional wall are monolithic. Eq. 2 is proposed to calculate the minimum additional wall length ratio β which the retrofitted THW element performs its ultimate capacity by yielding of all longitudinal rebars in the existing RC column when additional wall is under compression. For derivation of Eq.1 and Eq. 2, longitudinal rebars were modified to an idealized sandwiched section in the exiting RC column. The strain distribution diagram of THW element was divided into three regions (A, B and C) for the depth of neutral axis based on the stress state of longitudinal rebars. Every region was separated by a critical limit axial force ratio. After determination of all unknown factors in the section such as, the limit axial force ratios, axial force ratio within limits, the neutral axis depth and the stress state of longitudinal rebars in every region, Eq. 1 and Eq. 2 were derived as follows:

$$m = k_1 k_3 \kappa x_{n1}(0.5 + \beta - k_2 x_{n1}) + q(0.5 - d_{c1})(\gamma_t - \gamma_e) \quad (1)$$

$$\beta = \frac{1+u}{k_1 k_3 \kappa u}\{\eta + (1+\gamma)q\} - d_{c1} \quad (2)$$

Here, m = non-dimensional moment ($= M/bD^2F_c$), k_1,k_2 and k_3 = compressive stress block parameters, $\kappa = \sigma_{Badd}/F_c$, σ_{Badd} and F_c = concrete compressive strength of additional wall and existing RC column respectively, $q = p_t\sigma_y/F_c$, $p_t = a_t/(bD)$, a_t = cross section area of tension side rebars, b and D = width and depth of the RC column respectively, d_{c1} = d_c/D, d_c= distance between the RC column edge and the center of idealized sandwich reinforcement, $\gamma_t$and γ_e = tension and compression side rebars' stresses respectively, γ =$a_c/a_t = 1$, a_c = cross section area of compression side rebars, β = minimum additional wall length ratio, $u = E\varepsilon_{cu}/\sigma_y$, ε_{cu} = ultimate strain of concrete (0.003), E =Youngs's modulus of elasticity of rebars and η = acting axial force ratio.

In this section, the obtained ultimate flexural strength by Eq. 1 is compared with calculated results by the fiber model, simplified equation [5], Japan Building Disaster Prevention Association (JBDPA) equations [8, 9] and the experimental results as illustrated in Fig. 10. The experimental ultimate flexural strength is obtained in reverse from the experimental lateral strength V_{max} using Eq.3. The effectiveness of determining minimum additional wall length ratio β and its relationship with concrete compressive strength enhancement ratio κ is illustrated in Fig. 11.

$$_{THW}Mu = Qmu \cdot H + N \cdot \Delta - {}_cM_u \quad (3)$$

Where: $_{THW}M_u$ = moment at the bottom of THW section, Qmu =shear strength, H = height of specimen, $_cM_u$ = moment at top of existing RC column, N = acting axial force and Δ = displacement at the top of specimen. As is shown in Fig.10, the calculated flexural strength by the fiber model, simplified equation [5], the JBDPA [9] equation and experimental results verified the obtained results by Eq.1. According to these calculated and experimental results, all longitudinal rebars yielded in tension in the existing RC column when additional wall was under compression. The result of JBDPA [8] equation is lower compared to other results. According to JBDPA [8], the RC column with wing-wall performs its ultimate capacity by yielding of tensile longitudinal rebars. The fact that the experimental flexural strength verified the calculated results obtained by the fiber model, simplified equation [5] and proposed equation [6] indicates that the retrofitted THW elements behaved monolithic as it was assumed in these equations.

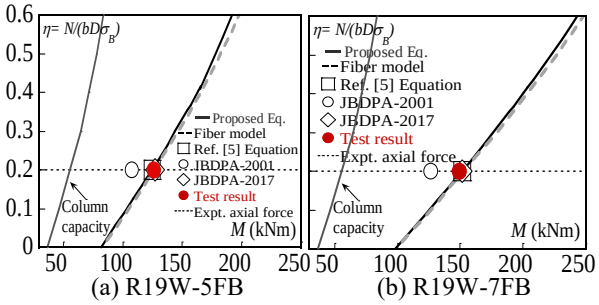

(a) R19W-5FB (b) R19W-7FB

Fig. 10 η-M interaction diagrams

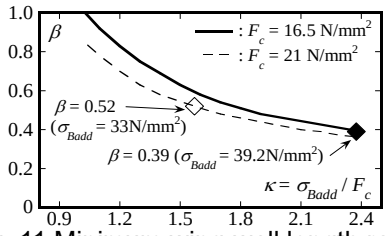

Fig. 11 Minimum wing-wall length ratio

The minimum additional wall length ratio (β = 0.52) was calculated based on the design strength of concrete (σ_{Badd} = 33 MPa, F_c = 21 MPa) by Eq. 2. Then, the specimens were constructed based on the value (β = 0.55) as minimum additional wall length ratio. The minimum additional wall length ratio become (β = 0.39) according to the test results of concrete (σ_{Badd} = 39.2 MPa, F_c = 16.5 MPa). It is evident from Fig. 11 that the value β decreases when compressive strength enhancement ratio ($\kappa = \sigma_{Badd}/F_c$) increases.

4. CONCLUSIONS

This investigation was conducted to verify the flexural strength and the experimental shear strength by the arch mechanism in the retrofitted THW element. The obtained results are concluded below.

(1) In bond specimens, longitudinal rebars yielded in tension in the existing RC column and breakage of rebars' was observed. In addition, the ultimate flexural strength increased due to the increment of additional wall length.

(2) The calculated and experimental results verify the accuracy of proposed equation and effectiveness of determining the minimum additional wall length ratio from the flexural strength aspects.

(3) The unbond specimens cracked diagonally under loading tests and performed their ultimate lateral strength by compressive failure of the diagonal strut. In addition, the ultimate shear strength was improved by increasing the additional wall length.

(4) The steel plates did not yield, and the confinement caused by the steel plates was small. Therefore, the resultant compressive force in bond specimens and the diagonal force of compressive strut in unbond specimens were not significantly affected by the lateral confinement caused by the steel plate.

ACKNOWLEDGMENT

The investigation reported herein was made possible by financial support in form of the Kajima Foundation's Research Grant and additional technical supports were provided by the Giken Co., Ltd. The authors hereby appreciate and acknowledge all these supports that ensured this research come out successful.

REFERENCES

[1] Yamakawa, T., Kamogawa S. and Kurashige, M.: An Experimental Study on the Seismic Retrofit Technique for RC Columns Confined with PC Bar Prestressing, Journal of Structural and Construction Engineering (Transaction of AIJ), No. 526, pp. 141-145, 1999.12 (in Japanese).

[2] Rahman, M. N. and Yamakawa, T.: Investigation of a Hybrid Technique for Seismic Retrofitting of Bare Frames, Journal of Advanced Concrete Technology, Vol. 5, No. 2, pp. 209-222, 2007.

[3] Nakada, K., Hitaka, T., Furukawa, A., Yamakawa, T. and Sakino, K.: Stress-strain Curve of RC Column Confined Externally by Pre-tensioned PC Bars, Journal of Structural and Construction Engineering (Transaction of AIJ), No. 600, pp. 147-153, 2006.2 (in Japanese).

[4] Nakada, K., Kuroki, M., Yamakawa, T. and Kikuchi, K.: Experimental Investigation of Shear Resistance Mechanism of an RC Column Externally Retrofitted with PC Bars, Journal of Structural and Construction Engineering (Transaction of AIJ), Vol. 82, No. 737, pp. 1071-1080, 2017.7 (in Japanese).

[5] Yamakawa, T., Javadi. P., Maeda, K. and Kobayashi, M.: Capacity-Based Analytical Evaluations of Retrofitted RC Frames -A New Hybrid Connection for Installation of a Steel Braced Frame Inside a RC Frame (Part 2)-, Journal of Structural and Construction Engineering (Transaction of AIJ), Vol. 75, No. 651, pp. 987-996, 2010.5.

[6] Nakada, K., Yamakawa, T., Javadi, P. Noori, MZ., Kaneda, K: Flexural Strength of the Strength-Ductility Type Seismic Retrofit Technique of RC Columns Using PC Bar Prestressing and Steel Plates, (Transaction of AIJ), Vol. 85, No. 767, pp. 97-104, Jan., 2020 (in Japanese).

[7] AIJ: Standard for Structural Calculation of Reinforced Concrete Structures, 1991 (in Japanese)

[8] The Japan Building Disaster Prevention Association: Standard for Seismic Evaluation of Existing Reinforced Concrete Buildings, 2001

[9] The Japan Building Disaster Prevention Association: Standard for Seismic Evaluation of Existing Reinforced Concrete Buildings, 2017 (in Japanese).

[10] Mander, J. B., Priestley, M. J. N. and Park, R.: Theoretical Stress-strain Model for Confined Concrete, J. of Structural Engineering, ASCE, Vol. 114, No. 8, pp. 1804-1826, 1988.8.